

Transport properties of Co in Cu(100) from first principles.

C. García Fernández,^{*,†} P. Abufager,[‡] and N. Lorente[¶]

[†]*Donostia International Physics Center (DIPC), Paseo Manuel de Lardizabal 4, 20018
Donostia-San Sebastián, Spain*

[‡]*Instituto de Física de Rosario, Consejo Nacional de Investigaciones Científicas y Técnicas
(CONICET) and Universidad Nacional de Rosario, Bv. 27 de Febrero 210 bis (2000)
Rosario, Argentina*

[¶]*Centro de Física de Materiales CFM/MPC (CSIC-UPV/EHU), Paseo Manuel de
Lardizabal 5, 20018 Donostia-San Sebastián, Spain*

E-mail: dr.carlos.garcia@dipc.org

Abstract

The electronic transport properties of a point-contact system formed by a single Co atom adsorbed on Cu (100) and contacted by a copper tip is evaluated in the presence of intra-atomic Coulomb interactions and spin-orbit coupling. The calculations are performed using equilibrium Green's functions evaluated within density functional theory completed with a Hubbard U term and spin-orbit interaction, as implemented in the Gollum package. We show that the contribution to the transmission between electrodes of spin-flip components is negative and scaling as λ^2/Γ^2 where λ is the SOC and Γ the Co atom-electrode coupling. Hence, due to this unfavorable ratio, SOC effects in transport in this system are small. However, we show that the spin-flip transmission component can increase by two orders of magnitude depending on the value of the Hubbard U term. These effects are particularly important in the contact regime because of the prevalence of d -electron transport, while in the tunneling regime, transport is controlled by the sp -electron transmission and results are less dependent on the values of U and SOC. Using our electronic structure and the elastic transmission calculations, we discuss the effect of U and SOC on the well-known Kondo effect of this system.

Introduction

The study of single magnetic atoms on non-magnetic metals has become a reality thanks to the advent of local scanning probe microscopies.^{1,2} This is a privileged situation in which precise measurements can be performed on a very controlled environment. Many theoretical works have been recently undertaken to quantitatively evaluate the properties revealed in these experiments.¹⁻³ Among these properties, Kondo physics^{4,5} is currently the object of much interest.⁶⁻¹³

Here, we take one of these almost-ideal systems and perform calculations to unravel the electronic structure and its effect on the electronic transport revealed by the experiments.

The system is a single Co impurity adsorbed on a Cu (100) surface that is contacted by a scanning tunneling microscope (STM) tip.^{8,9,11,12}

Many interesting effects have been found for this system. Polok and co-workers¹⁴ found that electron transport qualitatively changed with the tip-adatom distance. When the tip was far from the substrate, transport took place through the *sp*-induced electronic structure of the adatom. When the tip-apex atom approached until reaching covalent-bond distances, the electronic transmission involved the *d*-system. More curiously, the effect of the tip was a reordering of the electronic structure, changing the system's properties depending on the tip-surface distance. Unfortunately, these calculations did not address the very interesting Kondo physics experimentally revealed.^{11,12}

Direct calculations of the Kondo physics of Co on Cu (100) showed that the dynamical correlation processes were basically controlled by the d_{z^2} orbital of Co.¹⁵⁻¹⁷ Hence, the problem seemed to be greatly simplified by just considering the behavior of the d_{z^2} orbital as the tip-surface distance changed.¹⁸ However, all of these calculations were based on the results of plain density functional theory (DFT), which are known to underestimate the magnetic properties of adsorbed impurities. Particularly, two important ingredients present in modern calculations were missing from the above studies: the intra-atomic Coulomb interaction as given by the Hubbard U , and the spin-orbit coupling (SOC) of the Co atom.

In this work, we consider the effect of both interactions in the electronic structure of Co adatoms both in the tunneling regime that corresponds well to the Co / Cu (100) adsorbed system, and to the contact regime where the tip creates a covalent bond with the Co adatom becoming a point-contact junction. The paper contains a first section devoted to the methodology and setup of the calculations. We first show the results of the electronic structure and transmission calculations for different values of the Hubbard U . Next, the paper considers the effect of SOC in the Co atom and its influence on the electronic transmission. We analyze the electron transmission by simplifying the problem to the *d*-manifold of the Co atom and we rationalize the effect of SOC on the electron transmission in terms

of the strength of the SOC as compared to electronic coupling the Co d orbitals with the electrodes. We analyze the consequences of our findings on the Kondo effect and summarize the article.

Computational methodology

In this work, we depart from two of the reported optimized geometries of Choi et al.¹⁸ for an atomic junction formed by an adsorbed Co atom on a Cu(100) surface and a copper-covered tip. The two surfaces representing substrate and tip were modeled using a periodic slab geometry with a 3×3 surface unit cell, 6 layers for the surface holding the Co atom and 5 layers for the tip electrode.

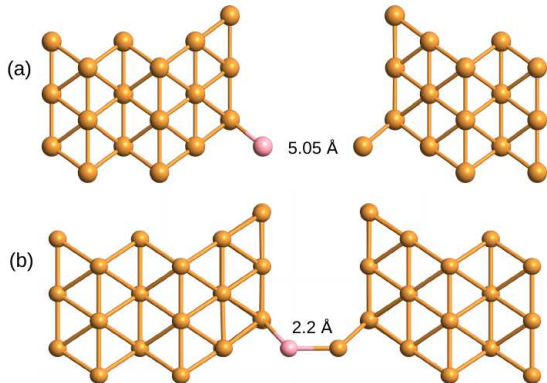


Figure 1: Atomic models with the two configurations used along this work:(a) the tunneling regime where the distance between the Co atom and the tip apex is 5.05 Å and (b) the contact regime where the same distance diminishes until typical covalent-bonding distances, here 2.2 Å. Periodic boundary conditions have been applied along the axes perpendicular to the transport direction.

DFT calculations have been performed within the spin-polarized generalized gradient approximation (GGA-PBE).¹⁹ Troullier-Martins full-relativistic pseudo-potentials,²⁰ an energy cutoff of 500 Ry and a $7\times 7\times 3$ K-point mesh generated according to the Monkhorst-Pack scheme, have been used in the Siesta code.²¹ A double- ζ plus polarization (DZP) basis set was defined to describe the Co and surface-atom electrons, while diffuse orbitals were used to improve the surface electronic description. Furthermore, a single- ζ plus polarization (SZP)

basis was set for the copper electrodes. Note that we employ a DZP basis set to describe the adsorbate states in order to yield correct transmission functions.²²

Quantum transport computations were performed from first-principles within the framework of the Landauer-Buttiker formalism. Thus, the DFT Hamiltonian and overlap matrices obtained with Siesta²¹ were analyzed in a post-processing step with the Gollum package.²³ This code is based on equilibrium transport theory and by carefully setting electrodes, branches and the central scattering region,²⁴ the transmission coefficients can be computed without performing independent selfconsistent calculations of the density matrix. This approach results in considerable savings of time and computational resources. Furthermore, one of the attractive features of Gollum is its functionality to compute spin transport in systems with spin-orbit interactions. Comparison with previous calculations¹⁸ using self-consistent non-equilibrium Green's function calculations shows that both calculations agree within the available numerical precision.

Results and discussion

Electronic structure and transport

The goal of the present section is to explore the sensitivity of the electronic and transport properties of the Cu-Co-Cu junction with respect to two distinct interactions: the Coulomb on-site repulsion, or Hubbard U , on Co- d orbitals and the spin-orbit coupling (SOC).

We first analyze the effect of the U parameter on the electronic and transport properties of the system comparing with the results of standard DFT (for the PBE exchange-and-correlation functional) in the tunnel Fig. 2 and contact regimes Fig. 3. Next, we include spin-orbit coupling and evaluate the same properties. We simplify the calculations to include just the d -electrons of the Co atom and rationalize our findings at the end of this section.

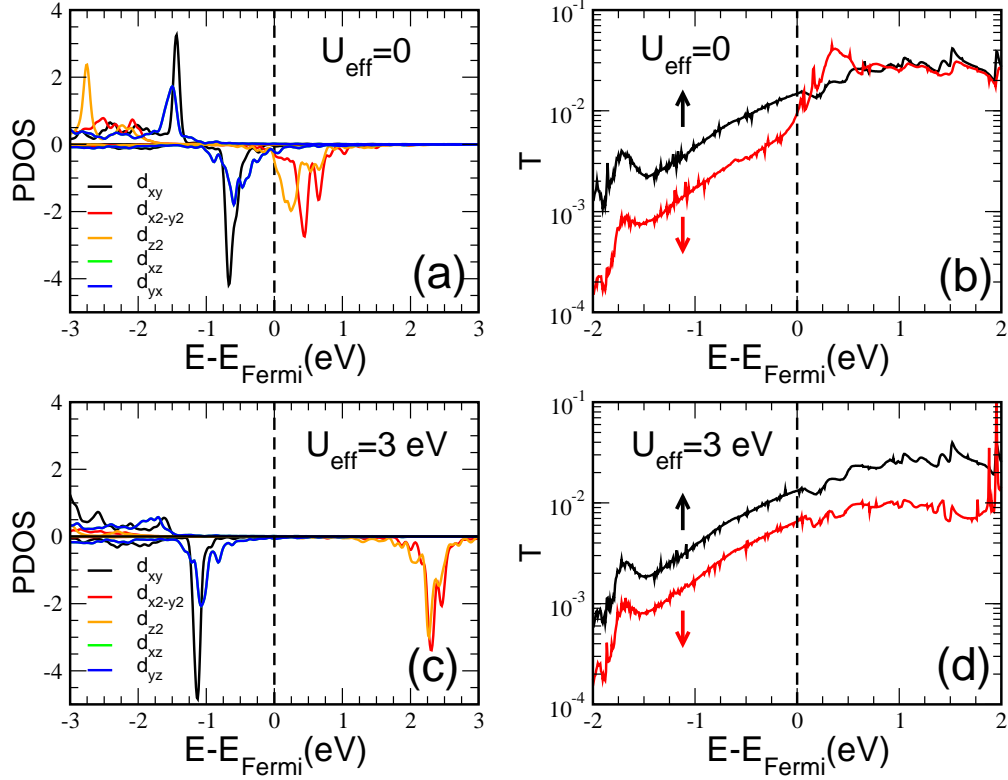


Figure 2: Results in the tunneling configuration for: (a,c) Density of states projected onto Co- d atomic orbitals (PDOS) and (b,d) electron transmissions (T) between electrodes as a function of electron energy referred to the Fermi energy ($E - E_{Fermi}$). No spin-orbit coupling is included and the graphs are divided in majority (positive PDOS and up arrow for T) and minority (negative PDOS and down arrow for T) spins. The Hubbard- U of the Co d -manifold used in the GGA+ U scheme are $U_{eff} = 0$ eV in the upper graphs (a,b), and $U_{eff} = 3$ eV in the lower ones, (c,d).

Effect of U on the electronic and transport properties

Fig. 2(a) and 3(a) shows the PDOS projected onto Co- d atomic orbitals, computed in this study without the inclusion of the Coulomb on-site repulsion, in the tunneling and contact configurations respectively.

When the tip is far from the cobalt atom, the two singly occupied $d_{z^2}, d_{x^2-y^2}$ magnetic orbitals are clearly shown as unoccupied states, in good agreement with the results by Polok *et al.*¹⁴ and Baruselli *et al.*¹⁵

However, the detailed electronic structure of the Co adatom changes in the contact region. There is a re-ordering of the minority spin d -states and contributions from d_{z^2} , d_{xz} and d_{yz}

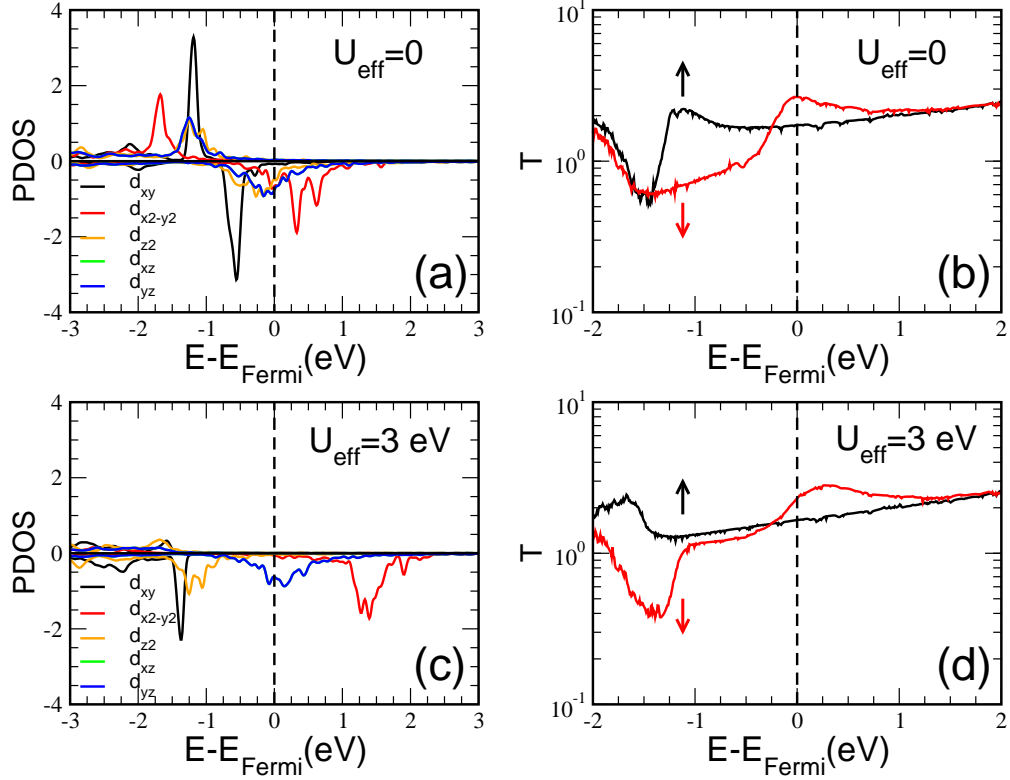


Figure 3: Results in the contact configurations for: (a,c) PDOS and (b,d) electron transmissions (T) with the same parameters and conventions as in Fig. 2.

orbitals become important at the Fermi level.^{14,18} In spite of the changes observed in the electronic structure, the overall magnetic properties slightly change since the Co adatom can be described as in a $3d^8$ ($S = 1$) configuration in both regimes.^{14–18,25}

The re-ordering of d levels in contact induces changes in the transport properties, as was previously reported.^{14,18} In the tunneling region, we find that transport Fig. 2 (b) basically takes place through the majority spin sp electrons of the Co atom.

In the contact regime, however, the d -electron contribution to the transmission at the Fermi level for the minority spin highly increases and the transport is governed by the minority spin channel. Indeed, the spin polarization defined as $P = (T_{\uparrow}(E_F) - T_{\downarrow}(E_F)) / (T_{\uparrow}(E_F) + T_{\downarrow}(E_F))$, where $T_{\sigma}(E_F)$ is the transmission per spin σ at the Fermi energy, changes its sign when going from tunneling to contact.

As reported before,^{14,18} our present calculations confirms the previous picture where

conduction takes place through the sp electrons of the Co adatom in tunneling while Co d -orbitals dominate the transport in the contact regime.

The Coulomb on-site repulsion on Co d -orbitals is an indispensable component in the above scenario. Since such interaction could modify the picture if the partially occupied d_{z^2} , d_{xz} and d_{yz} orbitals are pulled down with respect to unoccupied orbitals when U is increased. Here, we explore such an issue by performing LDA+ U calculations through the simplified rotationally invariant formulation of Dudarev et al,²⁶ with an effective $U_{eff} = U - J$ that includes the effect of the Fock exchange interaction, J . We use the implementation of the Siesta code.²⁷

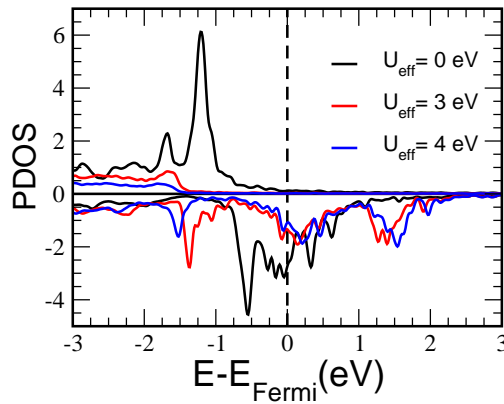


Figure 4: Spin-polarized PDOS projected onto Co($3d$) atomic orbitals at contact for $U_{eff} = U - J = 0, 3, 4$ eV

As depicted in Fig. 2(c) ($U_{eff} = 3$ eV) the overall properties for the tunnel regime slightly change with respect to the PDOS computed at the DFT level (Fig. 2(a)), being the main quantitative feature related to an increase of the energy separation among d -levels. However, when the tip is close to the surface Fig. 3(c), besides the separation among levels, the minority d_{z^2} is shifted to lower energies, leaving the d_{xz} and d_{yz} as the only orbital contributions around the Fermi energy. The increase of the separation among levels and the decrease of the minority channel contribution at the Fermi energy when including the Coulomb repulsion can be clearly seen in Fig. 4 depicting the total Co $3d$ PDOS for three different values of the effective U_{eff} .

In transport, a large Co *sp* contribution remains in the transmission at the Fermi level. As a result, good agreement is found between $U_{eff} = 0$ eV and $U_{eff} = 3$ eV calculations as can be seen from Figs. 2 (b) and (d). When the tip is near the surface adatom, two differences are clearly seen between $U_{eff} = 3$ eV (Fig. 3(d)) and $U_{eff} = 0$ eV (Fig. 3(b)). There is a shift in the energy scale, related to the new energy position of the Co orbitals. The second difference is an increase of 4% and 15% of $T(E_F)$ with respect to the $U_{eff} = 0$ values computed for the majority and minority spin channels, respectively. This difference can be traced back to a change in the d_{z^2} orbital energy.

In spite of these differences, the overall scenario of Refs.^{14,18} based on the leading transmission through the minority spin channel governed by Co-*d* orbitals remains unchanged. Therefore, we can conclude that the Coulomb on-site repulsion on Co-*d* orbitals does not have a strong effect on the transport properties of the Co junction.

Electronic transport in the presence of spin-orbit coupling

We include spin-orbit coupling (SOC) in the DFT equations following the implementations in Siesta²¹ and Gollum.²³ The PDOS, Fig. 5 (a) ($U_{eff} = 0$), reveals that the effect of SOC on the electronic structure of the Co-adatom is negligible within the accuracy of DFT calculations. This translates into the calculations of the electron transmission, showing that the presence of SOC produces no effect. Figure 5(b) compares the transmission with and without SOC. Both curves agree. However, the plotted total transmission is the sum of four terms. Mainly the direct non-spin-flip transmissions and the transmissions where the electron spin changes between electrodes. In the next section, we study the spin-flip contributions to the transmission and their sensibility to the Coulomb on-site repulsion.

Spin-orbit assisted spin-flip scattering

The present problem consists in a single center where the SOC is localized. We use the electronic structure computed above (with and without the inclusion of U_{eff}) to compute

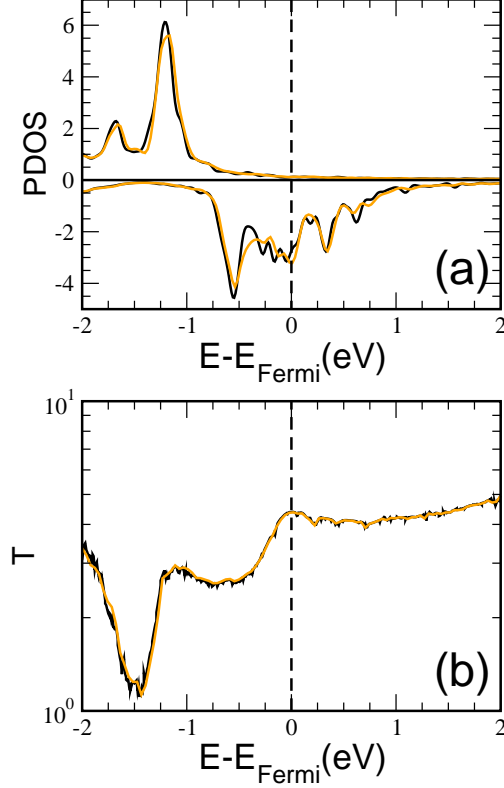


Figure 5: Total (a) PDOS projected onto Co(3d) atomic orbitals and (b) transmission at contact with (orange line) and without (black line) taking into account spin-orbit interactions and $U_{eff} = 0$.

the transmission by just considering the transmission through the d -orbitals that are the ones containing sizeable SOC contributions. This approximation is particularly well fitted to the contact regime. In Ref.¹⁸ three channels of strong d character are shown to dominate the transmission at contact while the sp channels dominate transport in the tunneling regime.

The transmission between electrodes for an electron injected at energy E through the d -orbitals of the Co atoms is:

$$T(E) = \sum_{i,j,k,l} \Gamma_{i,j}^L G_{j,k}^r \Gamma_{k,l}^R G_{l,i}^a. \quad (1)$$

Where i, j, k, l are indices over the spin orbitals of the d -electron manifold. The Green's functions $G_{j,k}^r$ and $G_{l,i}^a$ are the retarded and advance resolvents of the atomic Hamiltonian,

\hat{H} , in contact with the two electrodes, expressed again in the d -electron spin orbitals:

$$G_{j,k}^{r(a)} = \langle i | [E\hat{1} - \hat{H} - \hat{\Sigma}^{r(a)}]^{-1} | j \rangle. \quad (2)$$

The identity operator, $\hat{1}$, becomes a matrix of the dimension of the d manifold as well as the retarded (advanced) self-energy, $\hat{\Sigma}^{r(a)}$. The imaginary part of the self-energy is actually related to Γ of each electrode by (here i is the imaginary unit):

$$\hat{\Gamma} = i\hat{\Sigma}^r - i\hat{\Sigma}^a. \quad (3)$$

The total self-energy is the sum of self-energies due to each electrode.

In the spirit of the above calculations, we use Kohn-Sham orbitals, and the problem becomes a one-electron transport problem. From this analysis we find that for E between -2 and 2 eV transport at contact is dominated by three d orbitals in good agreement with previous results, Ref.¹⁸ Prior to switching on the SOC, we can identify the three spin orbitals as the minority spin degenerated d_{xz} and d_{yz} with some further contribution from the d_{z^2} orbital. This is particularly true for the $U_{eff} = 0$ cases, Figures 3 (a) and (b). The minority spin peak that dominates the transmission at the Fermi energy is clearly a contribution of the just mentioned orbitals. However, for $U_{eff} = 3$ eV, the d_{z^2} orbital shifts down in energy and the transmission at the Fermi energy is controlled by the minority-spin degenerated d_{xz} and d_{yz} . The comparison of Figs. 3 (a) and (c) show the clear reduction of the weight of d_{z^2} -type electronic structure at the Fermi energy. This is concomitant with the appearance of a sharp minimum at ~ -1.5 eV in Fig. 3 (d). Our calculations using the transmission through d orbitals, Eq. (1), show that its origin is a sizeable interference term $\Gamma_{z^2,xy}$ due to the mixing of orbitals by the Cu d -band that starts at ~ -1.8 eV.

The SOC is included in Hamiltonian, \hat{H} , restricted to the d -electron subspace. This is particularly simple to do in the Cartesian representation of d electrons. We follow Ref.,²⁸ where all matrix elements are carefully written. We write the SOC contribution to the

Hamiltonian as:

$$\begin{aligned}\hat{H}_{SOC} &= \lambda(\hat{L}_z\hat{S}_z + \hat{L}_x\hat{S}_x + \hat{L}_y\hat{S}_y) \\ &= \lambda(\hat{L}_z\hat{S}_z + \frac{1}{2}[\hat{L}_+\hat{S}_- + \hat{L}_-\hat{S}_+]).\end{aligned}\quad (4)$$

While the first term connects orbitals with the same $|m|$ and spin, where m is the eigenvalue of \hat{L}_z , the second term leads to spin-flips connecting spin-orbitals with different spins and orbitals of $|m \pm 1|$. If we consider the matrix elements in Cartesian terms, we also remark that while the matrix elements of $\hat{L}_z\hat{S}_z$ and $\hat{L}_x\hat{S}_x$ are purely imaginary, $\hat{L}_y\hat{S}_y$ are purely real. All diagonal matrix elements are zero because in Cartesian orbitals the average angular momentum is zero.

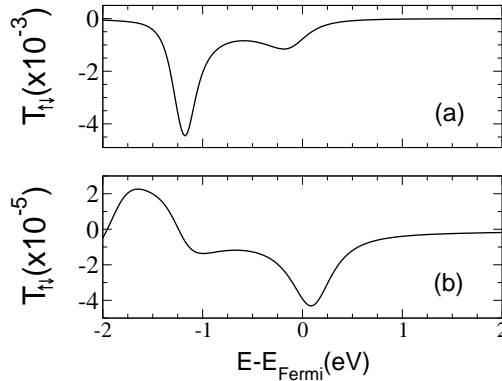


Figure 6: Spin-flip component of the transmission for (a) $U_{eff} = 0$ and (b) $U_{eff} = 3$ eV in the Co d -manifold. There is a factor-of-100 difference in the transmission between (a) and (b) marked in the y -axis label.

It is straightforward to build the new Green's function by inverting the old Hamiltonian with the above additional term, Eq. (4). The value we took for λ was the one of Co (I) because DFT yields a $3d^8$ state for Co ($S = 1$) in the contact configuration.¹⁸ Using the

values of Ref.²⁹ we have that $\langle \xi \rangle = 455 \text{ cm}^{-1}$, and

$$\lambda = \frac{\langle \xi \rangle}{2S} = 0.0284 \text{ eV}. \quad (5)$$

We retrieve our calculations using DFT with SOC for the transmission function, Fig. 5 (b), with the message that λ is so small that the effect on the transmission is negligible. As we will show in the next section, SOC effects will be noticeable as soon as the ratio $(\lambda/\Gamma)^2$ is not small, where Γ is the width of the d levels given by Eq. (3).

Since the spin of the electron in the electrodes is a good quantum number, we can study the transmission of each spin. From Eq. (1), we single out the spins and follow the transmission of each spin. We see that the transmission is a 2×2 matrix in spin due to the combinations of entering with either up or down spins and exiting with up and down including cross terms where the spin flips due to the presence of SOC at the Co atom. Let us analyze the spin-flip term:

$$T_{\uparrow,\downarrow}(E) = Tr[\Gamma_{\uparrow}^L G_{\uparrow,\downarrow}^r \Gamma_{\downarrow}^R G_{\downarrow,\uparrow}^a]. \quad (6)$$

Tr stands for trace over d orbitals and there are three matrix products because both Γ 's and G 's are matrices on d orbitals.

Figure 6 shows the results for the spin-flip transmission, $T_{\uparrow,\downarrow}(E)$ of Eq. (6). This contribution is negative, leading to the decrease of electron transmission in the system and to the increase of electron backscattering. Despite their small value stemming from the smallness of λ/Γ , we see fundamental differences between the two plotted cases. Figure 6(a) is the $U_{eff} = 0$ case while Fig. 6(b) is the $U_{eff} = 3 \text{ eV}$ one. The difference of two orders of magnitude between the two cases comes from the different electronic structure. In the $U_{eff} = 0$ case, the three orbitals d_{z^2} , d_{xz} and d_{yz} are close in energy about the Fermi level. These three orbitals have non-zero spin-orbit matrix elements connecting them because of the above spin-flip rule. Namely, the flipping of an electron leads to the change of $|m|$ where

m is the third component of the angular momentum of the spherical harmonics entering the orbital. Spin-flip then involves matrix elements changing $|m|$ by one, which is the case between the degenerated d_{xz} and d_{yz} with the $m = 0$, d_{z^2} orbital. When $U_{eff} = 3$ eV, the d_{z^2} orbital moves by more than 1.5 eV away from the d_{xz} and d_{yz} orbitals, quenching the spin-flip probabilities.

Simplified spin-orbit transmission

It is interesting to simplify the above treatment to enhance our insight into the spin-orbit-induced spin flip. Let us assume a single d orbital. In this case the spin-orbit contribution to the Hamiltonian becomes:³⁰

$$\hat{H}_{SOC} = i\lambda(\hat{d}_{\uparrow}^{\dagger}\hat{d}_{\downarrow} - \hat{d}_{\downarrow}^{\dagger}\hat{d}_{\uparrow}). \quad (7)$$

This is obviously Hermitian, and the matrix element is $i\lambda$, purely imaginary.

We adopt the broken-symmetry description of DFT, then, the atomic level becomes ϵ_{\uparrow} and $\epsilon_{\downarrow} = \epsilon_{\uparrow} + U$ with U the Hubbard charging energy. Within the wide-band approximation, the Green's function of the orbital in contact with two electrodes is:

$$G(E) = \begin{pmatrix} E - \epsilon_{\uparrow} + i\frac{\Gamma_{\uparrow}^L + \Gamma_{\uparrow}^R}{2} & -i\lambda \\ i\lambda & E - \epsilon_{\downarrow} + i\frac{\Gamma_{\downarrow}^L + \Gamma_{\downarrow}^R}{2} \end{pmatrix}^{-1} \quad (8)$$

with obvious notations for the self-energies of the level due to the left and right electrodes (real parts are strictly zero in the wide-band approximation) for each spin. Replacing these quantities in Eq. (1), we obtain for the direct terms:

$$T_{\uparrow,\uparrow}(E) = \frac{\Gamma_{\uparrow}^L \Gamma_{\uparrow}^R |E - \epsilon_{\downarrow} + i\frac{\Gamma_{\downarrow}^L + \Gamma_{\downarrow}^R}{2}|^2}{|(E - \epsilon_{\uparrow} + i\frac{\Gamma_{\uparrow}^L + \Gamma_{\uparrow}^R}{2})(E - \epsilon_{\downarrow} + i\frac{\Gamma_{\downarrow}^L + \Gamma_{\downarrow}^R}{2}) - \lambda^2|^2} \quad (9)$$

In the limit $\lambda \rightarrow 0$ we retrieve the usual result:

$$T_{\uparrow,\uparrow}(E) = \frac{\Gamma_{\uparrow}^L \Gamma_{\uparrow}^R}{|E - \epsilon_{\uparrow} + i \frac{\Gamma_{\uparrow}^L + \Gamma_{\uparrow}^R}{2}|^2}. \quad (10)$$

The spin-flip term is proportional to λ^2 :

$$T_{\uparrow,\downarrow}(E) = \frac{\Gamma_{\uparrow}^L \Gamma_{\downarrow}^R (i\lambda)^2}{|(E - \epsilon_{\uparrow} + i \frac{\Gamma_{\uparrow}^L + \Gamma_{\uparrow}^R}{2})(E - \epsilon_{\downarrow} + i \frac{\Gamma_{\downarrow}^L + \Gamma_{\downarrow}^R}{2}) - \lambda^2|^2}. \quad (11)$$

In the limit of large $\Gamma^R \sim \Gamma^L \sim \Gamma \gg \epsilon_{\uparrow}$ we see that the spin-flip contribution to the transmission becomes a negative quantity quadratic on the λ to Γ ratio:

$$T_{\uparrow,\downarrow}(E) \sim -\frac{\lambda^2}{\Gamma^2}. \quad (12)$$

This sets a scale for the values of λ that yield sizeable spin-flip terms in electron transport. Typically Γ is about a few hundred meV. If λ is in the tens of meV (*3d* transition metals) the spin-flip terms will be negligible in transport for a single scattering center. However, heavy elements will produce important spin-flips in point contacts.

Kondo effect

The computed electronic structure has direct bearings on the Kondo effect that a Co impurity displays in contact with copper electrodes.¹⁵⁻¹⁷ The very different electronic properties of the calculations of Figs. 2 (a) and (c) depending on the value of the Hubbard U , will change the interpretation of this Kondo effect. Indeed, for $U_{eff} = 0$, Fig. 2 (a) is in perfect agreement with the analyses published in Refs.,¹⁵⁻¹⁷ leading to the conclusion that the S=1 Kondo effect is actually a two-stage Kondo, where initially a S=1/2 Kondo effect is produced by the d_{z^2} -orbital charge fluctuations and the remaining magnetic moment gets screened at lower temperatures, driven by the charge fluctuations of the $d_{x^2-y^2}$ orbital.

The above picture is qualitatively the same as U increases, Fig. 2 (c). Although the

quantitative details will strongly vary. This is in agreement with the discussion by Baruselli *et al.*¹⁵ on the values of the computed Kondo temperatures pointing out the many difficulties to estimate accurate values based on DFT calculations.

At contact the picture radically changes. Figures 3 (a) and (c) show the half-occupied $d_{x^2-y^2}$ orbital leads to a $S=1/2$ Kondo effect. The d_{z^2} orbital is not relevant for Kondo physics anymore because it becomes completely occupied. The rest of the magnetic moment is screened by the charge fluctuations of a mixed-valence regime driven by the degenerate d_{xz} and d_{yx} orbitals. Qualitatively, the inclusion of U does not change the discussion although the final values will greatly differ.

The above results show that the Kondo effect of Co in contact with Cu electrodes can be considered as a single-orbital Kondo effect, at least for a large range of temperatures in the tunneling regime, and probably for all temperatures at contact. In this last case, non-equilibrium effects have been discussed before.¹⁸ The main effect at contact is the increased coupling to the electrodes given by Γ . The intrinsically non-equilibrium effects (bias-induced decoherence and peak splitting) are largely absent from the conductance behavior in the contact regime.¹⁸

The effect of spin-orbit interactions in Kondo processes has been much debated in the literature. Most works refer to the influence of a Rashba-like spin-orbit interaction on the Kondo spin-flip processes. The debate was very much calmed by the work of Meir and Wingreen³¹ showing that due to the preservation of time-reversal symmetry by the spin-orbit interaction, Kramers degeneracy is maintained and the Kondo processes are not affected. Recent works actually show that Rashba effects can change the Kondo temperature reducing it^{32,33} or increasing it³⁴ depending on the system.

Indeed, the effect of the environment is very important. Újsághy and co-workers^{35,36} showed that SOC can lead to sizeable magnetic anisotropies depending on the environment. This has important consequences for local spins larger than $1/2$, because it reduces the spin degeneracy and prevents Kondo spin-flip processes. Here, we are considering the local SOC

of a single impurity and not the extended Rashba-like interactions. Since the mean-field spin of cobalt is close to 1, we expect to find the disruptions caused by an emerging anisotropy due to SOC and the environment of the Co atom. However, our calculation yields a very small magnetic anisotropy energy (MAE) when a Co atom is adsorbed on the Cu (100) surface. The MAE is ~ 2 meV. Dividing by the Boltzmann constant yields a MAE ~ 23 K much smaller than $T_K \sim 90$ K, the Kondo temperature of Co on Cu (100).^{11,12,37} Hence, we do not expect any effect of the SOC in the tunneling regime. When the tip contacts the impurity, we find that the symmetry of environment of the Co atom increases, further reducing MAE to ~ 0.03 meV and unaffected the Kondo physics.

Conclusions

Electron transport through a Co atom between an STM tip and a Cu (100) substrate is shown to be largely independent of the Hubbard U values used in the evaluation of the electronic structure. Despite the dramatic effects of the inclusion of correlation, transport at the Fermi energy is basically controlled by the same orbitals. When the tip is far from the substrate, the tunneling regime is led by cobalt's sp -electronic structure. At contact, the d -electronic structure controls all electronic transport properties. Surprisingly, the electronic transmission with or without Hubbard U for both transport regimes is qualitatively the same and to a large extent also quantitatively.

The inclusion of spin-orbit coupling (SOC) does not change the quantitative values of transmission. We show that this is due to the small λ/Γ ratio, where λ is the SOC values and Γ is the Co electronic coupling to the electrodes. Transport with spin-orbit interactions gives rise to spin-flip processes. At lowest-order in the above ratio we find that the spin-flip component of the transmission is $T_{\uparrow,\downarrow}(E) \sim -\lambda^2/\Gamma^2$. Hence, for Co in metals this value is very small, but for heavier impurities will lead to sizeable decreases of electron transmission.

The effect of the Hubbard U in the spin-orbit induced spin-flip transmission is dramatic.

This is due to the shifting of critical orbitals to be able to complete a spin-flip process. Indeed the non-zero matrix elements of the SOC involve $\Delta S_z = \pm 1$ and $\Delta m = \pm 1$ states, where S_z and m correspond to the spin and orbital-angular moment. When the values of U_{eff} are ramped from zero to 3 eV, the $\Delta m = \pm 1$ states effectively split, reducing in two orders of magnitude the spin-flip component of the electron transmission, $T_{\uparrow,\downarrow}$.

The Kondo effect is strongly affected by the values of the Hubbard U although the qualitative picture gleaned in previous works¹⁵⁻¹⁸ remains unchanged. Moreover, we find that the Co SOC leads to small magnetic anisotropy energies, well below the typical Kondo temperatures, bearing no effect on Kondo processes for any of the conductance regimes analyzed here.

Acknowledgement

We thank Jaime Ferrer, Pablo Rivero and Salva Barraza for providing us with their cobalt pseudopotential. We further thank Jaime Ferrer for providing us with a copy of Gollum and for instructing us on its use. We thank Roberto Robles for many discussions and ideas. We gratefully acknowledge support from MINECO (Grant No. MAT2015-66888-C3-2-R), FEDER funds, the CCT-Rosario Computational Center and CONICET.

References

- (1) Gauyacq, J.-P.; Lorente, N.; Novaes, F. D. Excitation of local magnetic moments by tunneling electrons. *Progress in Surface Science* **2012**, *87*, 63 – 107.
- (2) Ternes, M. Probing magnetic excitations and correlations in single and coupled spin systems with scanning tunneling spectroscopy. *Progress in Surface Science* **2017**, *92*, 83 – 115.

- (3) Delgado, F.; Fernández-Rossier, J. Spin decoherence of magnetic atoms on surfaces. *Progress in Surface Science* **2017**, *92*, 40 – 82.
- (4) Kondo, J. Resistance Minimum in Dilute Magnetic Alloys. *Progress of Theoretical Physics* **1964**, *32*, 37–49.
- (5) Hewson, A. C. *The Kondo Problem to Heavy Fermions*; Cambridge studies in magnetism; Cambridge University Press, 1993.
- (6) Li, J.; Schneider, W.-D.; Berndt, R.; Delley, B. Kondo Scattering Observed at a Single Magnetic Impurity. *Phys. Rev. Lett.* **1998**, *80*, 2893–2896.
- (7) Madhavan, V.; Chen, W.; Jamneala, T.; Crommie, M. F.; Wingreen, N. S. Tunneling into a Single Magnetic Atom: Spectroscopic Evidence of the Kondo Resonance. *Science* **1998**, *280*, 567–569.
- (8) Knorr, N.; Schneider, M. A.; Diekhöner, L.; Wahl, P.; Kern, K. Kondo Effect of Single Co Adatoms on Cu Surfaces. *Phys. Rev. Lett.* **2002**, *88*, 096804.
- (9) Néel, N.; Kröger, J.; Limot, L.; Palotas, K.; Hofer, W. A.; Berndt, R. Conductance and Kondo effect in a controlled single-atom contact. *Phys. Rev. Lett.* **2007**, *98*, 016801.
- (10) Ternes, M.; Heinrich, A. J.; Schneider, W.-D. Spectroscopic manifestations of the Kondo effect on single adatoms. *Journal of Physics: Condensed Matter* **2009**, *21*, 053001.
- (11) Vitali, L.; Ohmann, R.; Stepanow, S.; Gambardella, P.; Tao, K.; Huang, R.; Stepanyuk, V. S.; Bruno, P.; Kern, K. Kondo Effect in Single Atom Contacts: The Importance of the Atomic Geometry. *Phys. Rev. Lett.* **2008**, *101*, 216802.
- (12) Choi, D.-J.; Rastei, M. V.; Simon, P.; Limot, L. Conductance-Driven Change of the Kondo Effect in a Single Cobalt Atom. *Phys. Rev. Lett.* **2012**, *108*, 266803.

- (13) Choi, D.-J.; Guissart, S.; Ormaza, M.; Bachellier, N.; Bengone, O.; Simon, P.; Limot, L. Kondo Resonance of a Co Atom Exchange Coupled to a Ferromagnetic Tip. *Nano Letters* **2016**, *16*, 6298–6302.
- (14) Polok, M.; Fedorov, D. V.; Bagrets, A.; Zahn, P.; Mertig, I. Evaluation of conduction eigenchannels of an adatom probed by an STM tip. *Phys. Rev. B* **2011**, *83*, 245426.
- (15) Baruselli, P. P.; Requist, R.; Smogunov, A.; Fabrizio, M.; Tosatti, E. Co adatoms on Cu surfaces: Ballistic conductance and Kondo temperature. *Phys. Rev. B* **2015**, *92*, 045119.
- (16) Jacob, D. Towards a full ab initio theory of strong electronic correlations in nanoscale devices. *Journal of Physics: Condensed Matter* **2015**, *27*, 245606.
- (17) Frank, S.; Jacob, D. Orbital signatures of Fano-Kondo line shapes in STM adatom spectroscopy. *Phys. Rev. B* **2015**, *92*, 235127.
- (18) Choi, D.-J.; Abufager, P.; Limot, L.; Lorente, N. From tunneling to contact in a magnetic atom: The non-equilibrium Kondo effect. *The Journal of Chemical Physics* **2017**, *146*, 092309.
- (19) Perdew, J. P.; Burke, K.; Ernzerhof, M. Generalized Gradient Approximation Made Simple. *Phys. Rev. Lett.* **1996**, *77*, 3865–3868.
- (20) Troullier, N.; Martins, J. L. Efficient Pseudopotentials for Plane-Wave Calculations. *Phys. Rev. B* **1991**, *43*, 1993.
- (21) Soler, J. M.; Artacho, E.; Gale, J. D.; García, A.; Junquera, J.; Ordejón, P.; Sánchez-Portal, D. The SIESTA method for ab initio order- N materials simulation. *Journal of Physics: Condensed Matter* **2002**, *14*, 2745.
- (22) Abufager, P. N.; Robles, R.; Lorente, N. FeCoCp₃ Molecular Magnets as Spin Filters. *The Journal of Physical Chemistry C* **2015**, *119*, 12119–12129.

- (23) Ferrer, J.; Lambert, C. J.; Garca-Suarez, V. M.; Manrique, D. Z.; Visontai, D.; Oroszlany, L.; Rodriguez-Ferradas, R.; Grace, I.; Bailey, S. W. D.; Gillemot, K. et al. GOLLUM: a next-generation simulation tool for electron, thermal and spin transport. *New Journal of Physics* **2014**, *16*, 093029.
- (24) GOLLUM 1.1: User Manual. *GOLLUM 1.1: User Manual* **2015**, , .
- (25) Surer, B.; Troyer, M.; Werner, P.; Wehling, T. O.; Lauchli, A. M.; Wilhelm, A.; Lichtenstein, A. I. Multiorbital Kondo physics of Co in Cu hosts. *Phys. Rev. B* **2012**, *85*, 085114.
- (26) Dudarev, S. L.; Botton, G. A.; Savrasov, S. Y.; Humphreys, C. J.; Sutton, A. P. Electron-energy-loss spectra and the structural stability of nickel oxide: An LSDA+U study. *Physical Review B* **1998**, *57*, 1505.
- (27) Wierzbowska, M.; Sanchez-Portal, D.; Sanvito, S. Different origins of the ferromagnetic order in (Ga,Mn)As and (Ga,Mn)N. *Phys. Rev. B* **2004**, *70*, 235209.
- (28) Dai, D.; Xiang, H.; Whangbo, M.-H. Effects of spin-orbit coupling on magnetic properties of discrete and extended magnetic systems. *Journal of Computational Chemistry* **2008**, *29*, 2187–2209.
- (29) Dai, D.; Whangbo, M.-H. Analysis of the Uniaxial Magnetic Properties of High-Spin d6 Ions at Trigonal Prism and Linear Two-Coordinate Sites: Uniaxial Magnetic Properties of Ca₃Co₂O₆ and Fe[C(SiMe₃)₃]₂. *Inorganic Chemistry* **2005**, *44*, 4407–4414.
- (30) Wilhelm, J.; Walz, M.; Evers, F. Ab initio. *Phys. Rev. B* **2015**, *92*, 014405.
- (31) Meir, Y.; Wingreen, N. S. Spin-orbit scattering and the Kondo effect. *Phys. Rev. B* **1994**, *50*, 4947–4950.

- (32) Žitko, R.; Bonča, J. Kondo effect in the presence of Rashba spin-orbit interaction. *Phys. Rev. B* **2011**, *84*, 193411.
- (33) Yanagisawa, T. Kondo Effect in the Presence of Spin-Orbit Coupling. *Journal of the Physical Society of Japan* **2012**, *81*, 094713.
- (34) Zarea, M.; Ulloa, S. E.; Sandler, N. Enhancement of the Kondo Effect through Rashba Spin-Orbit Interactions. *Phys. Rev. Lett.* **2012**, *108*, 046601.
- (35) Újsághy, O.; Zawadowski, A.; Gyorffy, B. L. Spin-Orbit-Induced Magnetic Anisotropy for Impurities in Metallic Samples of Reduced Dimensions: Finite Size Dependence in the Kondo Effect. *Phys. Rev. Lett.* **1996**, *76*, 2378–2381.
- (36) Újsághy, O.; Zawadowski, A. Spin-orbit-induced magnetic anisotropy for impurities in metallic samples. II. Finite-size dependence in the Kondo resistivity. *Phys. Rev. B* **1998**, *57*, 11609–11622.
- (37) Néel, N.; Kröger, J.; Limot, L.; Palotas, K.; Hofer, W. A.; Berndt, R. Conductance and Kondo Effect in a Controlled Single-Atom Contact. *Phys. Rev. Lett.* **2007**, *98*, 016801.